IOP Conf. Series: Journal of Physics: Conf. Series **847** (2017) 012045 doi:10.1088/1742-6596/847/1/012045

In vivo verification of particle therapy: how Compton camera configurations affect 3D image quality

D Mackin[1], E Draeger[2], S Peterson[3], J Polf[2] and S Beddar[1]
[1]The Department of Radiation Physics, University of Texas MD Anderson Cancer Center, 1515 Holcombe Boulevard, Unit 94, Houston, Texas 77030, USA
[2]The Department of Radiation Oncology, University of Maryland School of Medicine, Baltimore MD 21201, USA
[3]The Department of Physics, University of Cape Town, Rondebosch 7700, South Africa

Email: dsmackin@mdanderson.org

Abstract. The steep dose gradients enabled by the Bragg peaks of particle therapy beams are a double edged sword. They enable highly conformal dose distributions, but even small deviations from the planned beam range can cause overdosing of healthy tissue or under-dosing of the tumour. To reduce this risk, particle therapy treatment plans include margins large enough to account for all the sources of range uncertainty, which include patient setup errors, patient anatomy changes, and CT number to stopping power ratios. Any system that could verify the beam range *in vivo*, would allow reduced margins and more conformal dose distributions. Toward our goal developing such a system based on Compton camera (CC) imaging, we studied how three configurations (single camera, parallel opposed, and orthogonal) affect the quality of the 3D images. We found that single CC and parallel opposed configurations produced superior images in 2D. The increase in parallax produced by an orthogonal CC configuration was shown to be beneficial in producing artefact free 3D images.

1. Introduction

Though many methods have been proposed for *in vivo* verification of particle therapy, most methods utilize the secondary radiation produced by nuclear scattering of the beam particles. Early research into treatment verification focused on post treatment PET imaging of the beta decay of ^{11}C and ^{15}O. Though this method can utilize commercial PET scanners, the positron emission is not closely correlated with the beam range, and it suffers from poor resolution due to biological washout [1, 2]. Prompt gamma (PG) radiation does not suffer from these limitations, and it has garnered more of the recent research attention. However, because of the high energy (2 – 8 MeV) of PG radiation, detection system designed for PET and SPECT are not suitable. Novel detection systems, designed for PG radiation emitted during particle therapy must be developed.

The purpose of our research is to develop a clinical imaging system capable of *in vivo* verification of the delivery of particle therapy treatments. To this end, we have been collaborating with H3D Inc. (An Arbor, Michigan, USA) to develop a custom, multi-stage cadmium, zinc, telluride (CZT) Compton camera (CC) gamma detection system and a novel image reconstruction algorithm capable of producing 3D images of gamma emission. In this article, we begin by describing the gamma emission produced during proton and the hardware components of our Compton camera, PolarisJ2. We next investigate how single camera, parallel opposed, and orthogonal CC configurations affect the quality of the reconstructed 3D images using both a back projection and an iterative reconstruction algorithm.

Content from this work may be used under the terms of the Creative Commons Attribution 3.0 licence. Any further distribution of this work must maintain attribution to the author(s) and the title of the work, journal citation and DOI.
Published under licence by IOP Publishing Ltd

IOP Conf. Series: Journal of Physics: Conf. Series **847** (2017) 012045 doi:10.1088/1742-6596/847/1/012045

2. Materials and Methods

2.1. The prompt gamma spectrum

The spectrum of the secondary particles produced by nonelastic scattering during particle therapy is complex. However, for PG verification of particle therapy, two gamma energies are of particular importance, 4.44 and 6.13 MeV which are excited nuclear states of carbon and oxygen respectively [3, 4]. These gammas are the most prevalent above 3 MeV, and the 6.13 MeV gamma ray emission is closely correlated with the Bragg peak.

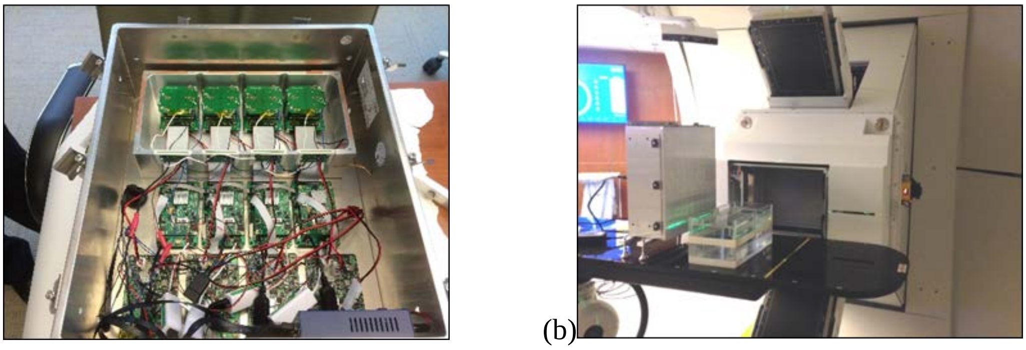

(a) (b)

Figure 1. (a) The inside of a single stage of a PolarisJ2 Compton camera. (b) A single PolarisJ2 CC stage in a proton therapy treatment vault.

2.2. The PolarisJ2 Compton Camera Imaging System

The PolarisJ2 from H3D (An Arbor, Michigan), has been updated from the PolarisJ system [5] to provide a larger detector volume and much faster readout. The current iteration of the detector consists of 2 independent detector stages, each with 4, 4x4 arrays of CZT crystals. Each crystal is pixelated into an 11x11 grid, and each pixel is read out independently by an application specific integrated circuit (ASIC) controlled a CPU running a Linux operating system. The four crystal arrays and controllers are shown in Fig. 1 (a). A single PolarisJ2 CC stage in a proton therapy treatment vault is shown in Fig. 1 (b).

2.3. Compton camera configurations and simulations

CC imaging systems rely on parallax to achieve resolution in the direction orthogonal to detector faces, and the finite width of the detector limits the orthogonal resolution [6]. One way to reduce this problem would be to simply make the detector much bigger. However, multiple smaller detectors may provide more parallax, and, therefore, higher quality images. For this study we simulated a 200 MeV proton beam on a water phantom using a Geant4.9.4 Monte Carlo model described in detail in [7]. The two simulated CC detector stages were $8\times8\times1$ cm^3 and centered 9.5 cm and 17.3 cm from isocenter. The simulations were performed multiple times with the Compton camera positioned at 0, 90, 180, and 270 degrees. The independent simulations were then combined to produce parallel opposed and orthogonal configurations. Each simulation used 2×10^9 particle histories.

To reconstruct the images we used a back projection algorithm that counts the intercepts between the Compton cones and the voxels in the region of reconstruction. We also used an iterative reconstruction algorithm derived based on stochastic origins ensembles method [8, 9]. Only two scatters were used for each detected gamma, and the energies were assumed to be either 4.44 MeV or 6.13 MeV. The known proton spot position was used as prior information for both reconstruction methods. All images were produced using 20k detected gammas.

3. Results

The back projection images are instructive because they visualize the raw information that is the input to the iterative reconstruction algorithm. In the top rows of Fig. 2 and Fig. 3, artifact of the Compton scatter cones projected away from the CC are apparent in the direction orthogonal to the CC.

IOP Conf. Series: Journal of Physics: Conf. Series **847** (2017) 012045 doi:10.1088/1742-6596/847/1/012045

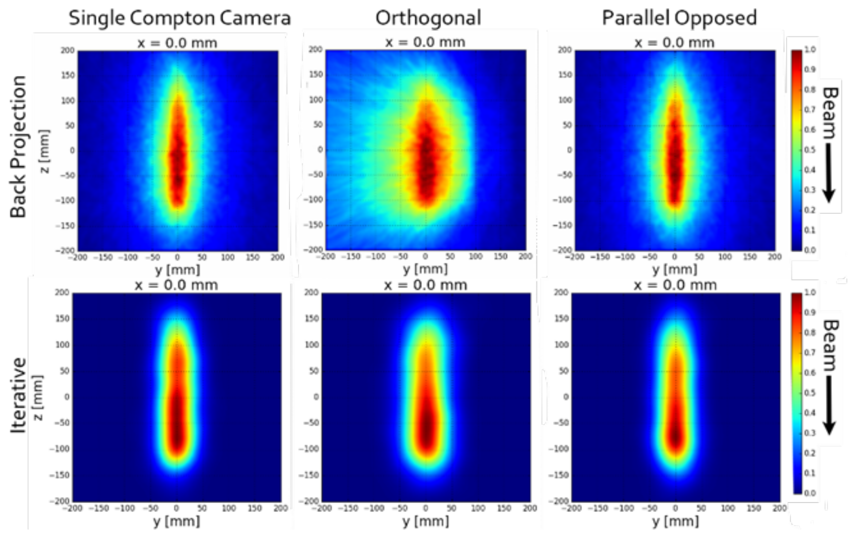

Figure 2. A comparison of 2D slice images of a simulated 200 MeV proton beam incident on a water phantom. The columns are three detector configurations: a single Compton camera (left), two Compton cameras aligned orthogonal to each other (middle), and parallel opposed (right). The rows show images created using back projection (top) and stochastic origin ensembles iterative (bottom) algorithms. The color scale represents relative gamma emission intensities.

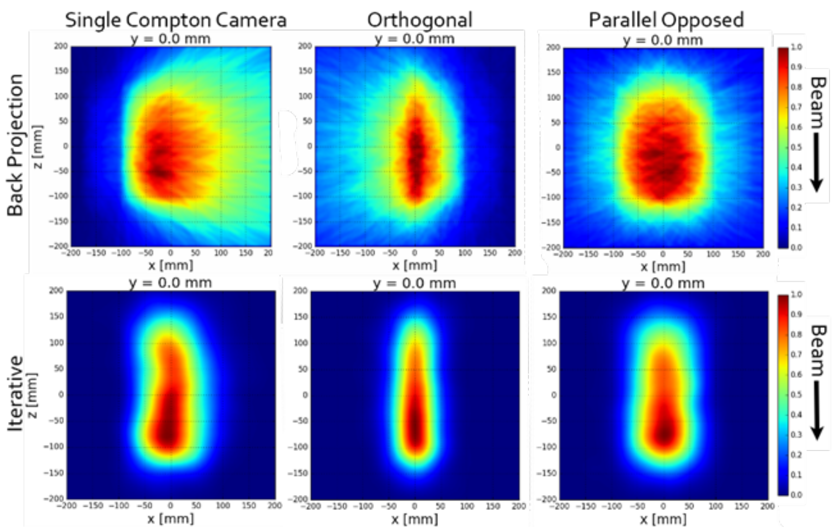

Figure 3. The same image comparison as Fig. 4 except that the x=0 plane has been replaced with the y=0 plane.

For the single and parallel opposed CC configurations, the artifacts appear only in the $y = 0$ plane, orthogonal to the detector faces (Fig. 3). For the orthogonal CC configuration, the artifacts appear in both planes (Fig. 2 and Fig 3, top rows). However, the parallax provided the orthogonal enables the iterative reconstruction to remove the artifacts in both planes (Fig. 2 and Fig 3, bottom rows). Due to the limited parallax in the $y = 0$ plane for the single and parallel opposed CC configurations, the iterative reconstruction produced an inaccurate curvature in the single CC images and a widening of the images in the parallel opposed configuration (Fig. 3, bottom row).

4. Discussion and Conclusions

We have demonstrated the effects of CC configuration on the 3D images of the PG emission for proton beams. Similar results can be expected for particle therapy beams except that the PG emission is much greater for heavier ions [10]. Practical considerations such as cost and physical space will limit the size and number of CCs that can be used in a particle therapy vault. However, we have demonstrated that the parallax information gained from multiple CCs can improve image quality. In this study, we focused on the increased parallax, and, therefore, we used equal numbers of detected gammas for each configuration. When used clinically, multiple detectors will also increase the number of gamma ray detections available for the image reconstruction. In this study, we looked only at beams along the central axis. Both the parallel opposed and orthogonal configurations are likely to show biases for beams that are closer to one CC than the other. These biases will have to be corrected as part of the image reconstruction.

There is not one ideal detector configuration for CC imaging systems. In this study, parallel opposed and single CC configurations produced superior back projection images in 2D. The increase in parallax provided by an orthogonal CC configuration was shown to be beneficial in producing artefact free 3D images.

5. References

[1] Knopf A *et al* 2008 *Phys. Med. Biol.* **53** 4137
[2] Parodi K *et al* 2007 *Int. J. Radiat. Oncol.* **68** 920-34
[3] Kozlovsky B *et al* 2002 *Astrophys. J. Suppl. S.* **141** 523
[4] Verburg J M *et al* 2012 *Phys. Med. Biol.* **57** 5459
[5] McCleskey M *et al* 2015 *Nucl. Instrum. Meth. A* **785** 163
[6] Maxim V 2014 *IEEE T. Image Process.* **23** 332-41
[7] Polf J C *et al* 2014 *Phys. Med. Biol.* **59** 2325
[8] Andreyev A *et al* 2011 *Med. Phys.* **38** 429
[9] Mackin D *et al* 2012 *Phys. Med. Biol.* **57** 3537 - 53
[10] Pinto M *et al* 2014 *Phys. Med. Biol.* **60** 565